Mid-latitude E-region bulk motions inferred from digital ionosonde and HF radar measurements

G. C. Hussey[1], C. Haldoupis[2], A. Bourdillon[3], J. Delloue[4], and J. T. Wiensz[1]

[1]Institute of Space and Atmospheric Studies, Department of Physics and Engineering Physics,
University of Saskatchewan, Saskatoon, Saskatchewan, Canada
[2]Physics Department, University of Crete, Iraklion, Crete, Greece
[3]Laboratoire IETR, Université de Rennes 1, Rennes, France
[4]Université Pierre et Marie Curie, Paris, France

LOGO

Mid-latitude E-region bulk motions inferred from digital ionosonde and HF radar measurements

G. C. Hussey[1], **C. Haldoupis**[2], **A. Bourdillon**[3], **J. Delloue**[4], **and J. T. Wiensz**[1]

[1]Institute of Space and Atmospheric Studies, Department of Physics and Engineering Physics, University of Saskatchewan, Saskatoon, Saskatchewan, Canada
[2]Physics Department, University of Crete, Iraklion, Crete, Greece
[3]Laboratoire IETR, Université de Rennes 1, Rennes, France
[4]Université Pierre et Marie Curie, Paris, France

Abstract. In the mid-latitude E-region there is now evidence suggesting that neutral winds play a significant role in driving the local plasma instabilities and electrodynamics inside sporadic-E layers. Neutral winds can be inferred from coherent radar backscatter measurements of the range-/azimuth-time-intensity (RTI/ATI) striations of quasi-periodic (QP) echoes, or from radar interferometer/imaging observations. In addition, neutral winds in the E-region can be estimated from angle-of-arrival ionosonde measurements of sporadic-E layers. In the present paper we analyse concurrent ionosonde and HF coherent backscatter observations obtained when a Canadian Advanced Digital Ionosonde (CADI) was operated under a portion of the field-of-view of the Valensole high frequency (HF) radar. The Valensole radar, a mid-latitude radar located in the south of France with a large azimuthal scanning capability of 82° (24° E to 58° W), was used to deduce zonal bulk motions of QP echoing regions using ATI analysis. The CADI was used to measure angle-of-arrival information in two orthogonal horizontal directions and thus derive the motion of sporadic-E patches drifting with the neutral wind. This paper compares the neutral wind drifts of the unstable E patches as determined by the two instruments. The CADI measurements show a predominantly westward aligned motion, but the measured zonal drifts are underestimated relative to those observed with the Valensole radar.

1 Introduction

Coherent radar backscatter studies of the unstable mid-latitude E-region have shown that sporadic-E layers (E_s) and neutral winds play a fundamental role in formulating the plasma physics unique to this region (*e.g.*, Riggin et al. (1986); Hussey et al. (1998); Hysell et al. (2002), among others). Sporadic-E layers drifting with the neutral wind provide patches of metallic ions needed for plasma instability

excitation while the neutral wind constitutes the source of free energy.

A recent radio interferometer study by Haldoupis et al. (2003), based on a large data base obtained with the Sporadic-E Scatter experiment (SESCAT) in Crete, Greece, showed that E_s echoes come from discrete plasma structures, presumably unstable E_s plasma patches or blobs, having a variety of zonal sizes ranging from a few kilometres to several tens of kilometres. The great majority of these structures drift with westward speeds between about 20 to 100 m/s, whereas values as high as 150 m/s are not uncommon. These predominately westward motions of sporadic-E patches have also been measured in several radar and rocket studies (*e.g.*, Tanaka and Venkateswaran (1982); Yamamoto et al. (1992); Bourdillon et al. (1995); Larsen et al. (1998), Haldoupis et al. (2001), Hysell et al. (2002), among several others). In their discussion, Haldoupis et al. (2003) suggested that the westward motions in sporadic-E backscatter is an inherent property of the phenomenon which might be of importance not only in creating the E_s layering (in accordance with the wind shear theory), but also in the destabilising process as well. The latter could happen directly, for example along the lines of the wind-driven instability mechanism of Kagan and Kelley (1998), or indirectly by setting up strong eastward electric fields which then can excite the gradient drift and/or the Farley-Buneman instability (*e.g.*, Haldoupis et al. (1997)).

Given the anticipated importance of the westward neutral winds in mid-latitude sporadic-E layer instabilities, the present paper aims in providing a further test of the neutral wind role on unstable E_s by comparing the bulk motions deduced from azimuth-time-intensity striations of the Valensole HF radar quasi-periodic echoes, and those from a CADI ionosonde with the ability to measure angle-of-arrival information of drifting E_s plasma structures. The Valensole radar is located in the south of France and has a large azimuthal coverage of 82° (from 24° east to 58° west), and thus is capable of measuring zonal bulk motions of unstable E_s patches as they drift horizontally with the wind across the field-of-

view of the radar. The CADI was observing a portion of the field-of-view of the HF radar for a time during the summer of 1995 when both systems were run concurrently. Here, the CADI drift measurements are compared, in an effort also to be validated, with those deduced by ATI plots of the Valensole radar.

2 The Experiments

The Valensole HF radar (43.8° N; 6.1° E geographic; 37.1° N; 82.2° E geomagnetic) has been utilised in a number of sporadic-E experiments (SPOREX) for studying coherent echoes from decametre wavelength irregularities over the last few years (e.g., Bourdillon et al. (1995); Haldoupis et al. (2001) and references therein).

During the summer of 1995 the radar was operated in a SPOREX mode and during the last phase of the experiment there was a CADI ionosonde operating under a part of the Valensole radar field-of-view. The CADI was located near the village of Termignon (45.3° N, 6.8° E geographic) about 175 km northeast of Valensole as shown in Figure 1. With respect to the radar field-of-view, the ionosonde was situated at an azimuth of 18.8° and at a range between 196 and 212 km, which corresponds to magnetic aspect sensitive backscatter heights between 90 and 120 km. In the 1995 campaign, the radar operated from the 27 May to 28 June, and from the 3 to 13 July, whereas the ionosonde operated only from the 4 to 17 July; therefore, there was only overlap in time of the two instruments from the 4 to 13 July.

2.1 Termignon CADI

The CADI measurement technique is based on the ionosonde Doppler drift or imaging Doppler interferometry (IDI) technique, which is described by Grant et al. (1995) and in more references therein. Basically, angle-of-arrival information, along with the normal amplitude (power) information, is determined from cross-spectral analysis of a pair of receiving antennas. The CADI used at Termignon consisted of four receivers and thus was able to measure angle-of-arrival information in two orthogonal directions. The transmitting antenna consisted of a delta antenna and the receiving array consisted of four dipoles arranged in a square with the sides aligned north-south (NS) and east-west (EW) geographically. The NS interferometer pair separation was 59.6 m and the EW separation was 60.0 m. The CADI was configured to make an ionogram sweep, which took ∼80 s, every 10 min and then a series of fixed frequency soundings at five frequencies, which took ∼32 s for all five fixed frequencies, over the next 6 minutes. The ionogram measurements were synchronised on 10 min boundaries beginning at 00 min of the hour and the fixed frequency measurements were nominally synchronised to the nearest minute. The ionogram sweep sounding operating parameters were a 4-point spectrum averaged over 4 pulses for 200 frequencies from 2 to 10 MHz. For the fixed frequency sounding a 64-point spectrum averaged over 4 pulses for the five frequencies 2.1, 2.6, 3.3, 4.2, and 5.2 MHz was used. For either configuration the pulses per second or pulse repetition rate was 40 Hz and the height (altitude) range was from 90 to 510 km with a resolution of 3 km.

The CADI is a low powered ionosonde and thus susceptible to man-made interference which is significant in the MF/HF bands in the European sector. This interference was reduced because the site at Termignon was located in a mountain valley; nonetheless, the interference was such that only strong reflections could be recognised as ionospheric soundings. To reduce interference effects, the Termignon CADI was modified by introducing a crystal filter at the IF (intermediate frequency) stage of the receivers. This reduced further, but did not eliminate, the interference which still could be seen in the ionograms, as for example in those presented in Figure 2.

2.2 Valensole HF radar

The Valensole HF radar consisted of several synchronised receivers and used beam forming techniques to cover a large azimuthal sector with good angular resolution. It used a wide-beam antenna for northward transmission (3-db beam width at 15 MHz was ∼ 60°) and a narrow beam 560 m long linear array of 48 vertical antenna elements for phased-array reception. At the receiver, a steering unit switched the array beam in steps of 12° over seven adjacent sectors each divided into 6 sub-sectors using digital beam forming. As such, a full azimuthal scan consisted of 42 elementary beams between 24° E and 58° W, each having a 3-db beam width of 2° at 15 MHz. In this configuration, for example, the radar covered a zonal distance of ∼ 320 km at the 200 km range.

In SPOREX 1995, the received signal was gated every 18 km to give 15 range-gates between 100 and 370 km. This satisfied the 0° aspect sensitivity condition for E-region altitudes between 90 and 130 km over a large ionospheric area centred near 37° invariant magnetic latitude, $L = 1.7$, and magnetic dip of ∼ 60°. Another capability of the system was the simultaneous radar operation in two or more pulse-to-pulse interlaced frequencies. An array processor was used for real time fast Fourier transform Doppler spectrum computations. For more details on the radar and its capabilities, see Bourdillon et al. (1995) and Six et al. (1996).

3 Data Presentation and Analysis

As shown in Figure 1, the experiment was designed to make overlapping observations of the field-of-views of the Valensole HF radar and the CADI ionosonde located at Termignon. In the paper by Haldoupis et al. (2001), the large azimuthal coverage of the Valensole HF radar was used to study quasiperiodic (QP) echoes in the zonal direction using azimuth-time-intensity (ATI) analysis. The slope of the striations of the ATI plots, which is reminiscent of those seen in range-time-intensity (RTI) plots of mid-latitude radars view-

ing a fixed azimuth about the meridian, could be used to infer bulk motion in the zonal direction across the radar field-of-view.

QP echoes, a coherent radar backscatter phenomena only observed in the summertime mid-latitude E-region ionosphere, are uniquely identified on RTI plots of northward viewing radars as sequential striations of backscatter with typical periods from a few minutes to ~ 20 min and range rates, dR/dt, from ~ 20 to 100 m/s. They were first reported by Yamamoto et al. (1991) using the Middle and Upper (MU) radar near Kyoto, Japan. It has been found that these field-aligned coherent echoes have a close association with sporadic-E layers and interferometer studies have indicated that they are restricted to typical lower E-region scattering altitudes associated with field-aligned coherent radar backscatter. The interferometer studies have also shown that these E_s plasma patches or blobs, which provide the plasma for irregularity excitation and subsequent coherent echoes, have sizes from a few to tens of kilometres and often, but not always, drift westward (*e.g.*, Riggin et al. (1986); Pan et al. (1994); Hussey et al. (1998); Hysell et al. (2002); Haldoupis et al. (2003), and others). The Valensole HF radar with its large range gates of 18 km has difficulty observing QP echoes in the NS or meridional direction (RTI analysis) as field-aligned backscatter at E-region altitudes typically is only observed in one or two range cells; however, the large azimuthal coverage of the radar allows for studying the QP echoes in the zonal direction (ATI analysis) as applied in this study and as first presented in Haldoupis et al. (2001).

The CADI ionosonde at Termignon measured angle-of-arrival information in two orthogonal directions and hence could estimate horizontal sporadic-E layer motions at E_s layer altitudes in the E-region. It is assumed that the motions observed are due to the neutral winds at these altitudes (~ 100 to 110 km), because the ions are strongly collisional and thus the plasma is dragged along with the neutrals.

As has been previously reported by Riggin et al. (1986) and Hussey et al. (1998) the presence of sporadic-E is essential in creating the conditions needed for excitation of plasma instabilities in the summertime mid-latitude E-region. These studies compared 50-MHz VHF coherent backscatter and co-incident and simultaneous electron density profile measurements and indicated a direct correlation with E_s electron densities $> 2 \times 10^5 \mathrm{cm}^{-3}$, which corresponds to a plasma or E_s frequency > 4 MHz, and the occurrence of coherent backscatter. Figure 2 presents a number of sequential ionograms clearly showing sporadic-E from 2220 to 2340 UT, inclusive, on 11 July, 1995. This E_s activity was also accompanied by coherent backscatter observed by the Valensole radar, which is to be presented shortly, for a slightly shorter period. Similar conditions, namely that E_s layers are always present when coherent backscatter is observed, are assumed to apply in this HF study as in the VHF studies. Although the majority of the sporadic-E observations in this study have peak frequencies > 4 MHz (6 to 8 MHz are typical), there are, however, cases where HF backscatter is observed and the peak E_s frequency is 3 to 4 MHz as can

be seen, for example, in Figure 2. Sporadic-E is a proxy for the ambient electron density gradients and these density gradients are directly involved in the irregularity excitation mechanism responsible for the backscatter. Weaker electron density gradients are sufficient for irregularity excitation at HF frequencies than at VHF frequencies and, as such, it is expected that lower peak E_s frequencies will correlate with HF coherent backscatter.

Since an ATI striation slope represents the bulk motion of an unstable plasma patch drifting in the azimuthal direction, then this patch is only observed simultaneously by both instruments where their fields-of-view overlap. In practice a CADI receives reflections from overhead within $\sim 30°$ of the zenith. As such, for altitudes associated with sporadic-E layers (typically 100–110 km), this corresponds to a field-of-view diameter of ~ 100 km. On the other hand, the full azimuthal extent of the radar at a range of 174 km is ~ 250 km and the ATI striations never cover the entire azimuthal extent. This suggests that the field-of-view of the CADI covers at a minimum 40%, and typically much more, of the field-of-view of the HF radar at the radar ranges and azimuths of interest. This, as well as the assumption that the motion is controlled by the ambient neutral wind, which should not change significantly in the time periods under consideration, allows for the tacit assumption that both instruments are viewing approximately the same region in space.

As mentioned, the overlap in time of the two instruments was from the 4 to 13 July, 1995. Since HF echoes are a subset of E_s observations, the cases where striations were observed on ATI plots were first selected. Note that striated echoes means structured layers with unstable E_s patches moving in sequence across the radar field-of-view. Typical ATI analysis will be presented in the next section followed by the corresponding CADI observations in the subsequent one.

3.1 Valensole HF Radar Observations

The search for striations on Valensole ATI plots resulted in 8 clearly defined events. A typical event is presented in Figure 3 for the radar frequency of 11.03 MHz. The radar operated in a four-frequency mode for the 1995 campaign (*e.g.*, Hussey et al. (1997); Haldoupis et al. (1998)) in order to study the wavelength dependence of decametre-scale plasma irregularities. However, the present study only requires a single frequency and thus the 11.03 MHz frequency (irregularity wavelength of 13.6 m) was selected since it was less afflicted with man-made interference and because in general received echoes more often than the 9.23, 12.71 and 16.09 MHz frequencies.

Figure 3 shows the power or intensity plots for two consecutive radar ranges, 174 and 192 km, where the 11.03 MHz echoes are usually located because of ray bending due to refraction. Ray bending can be significant at mid-latitudes when E_s is present as shown in Hussey et al. (1999) and Haldoupis et al. (2001). The ordinate of the plots presents the complete azimuthal extent of the radar ($24°$ to $-58°$), while the abscissa presents time (~ 2200 to 0002 UT on the night

of 11–12 July, 1995). The radar took ∼4 min to complete a scan and the plotted intensity colour-scale was smoothed using cubic convolution interpolation.

The thick black lines plotted on both the 174 and 192 km range plots in Figure 3 are drawn in order to exemplify the ATI striations. As mentioned, the azimuths scanned by the radar range from 24° east to 58° west with the ATI striations here starting at ∼2230 UT in the east and ending at ∼2329 UT in the west, thus the bulk motion inferred from the positive slope lines was roughly 37 m/s westward at the 174 km range and 35 m/s westward at the 192 km range giving an average value of 36 m/s westward. The motion is along the contours of magnetic aspect sensitivity, which essentially is aligned in the zonal direction (actually it is ∼10–15° to the southwest of east) as the boresight of the radar is aligned with geographic north (see Figure 1). Unfortunately, there were no cases of eastward motions, or negative striation slopes, in the present data set. These usually identify with early morning hour echoes which occur significantly less often than the frequent pre-midnight echoes which always associate with westward bulk motions (*e.g.*, Bourdillon et al. (1995); Haldoupis et al. (2001)).

As represented by the plots in Figure 3, the striations are typically seen on the most aspect sensitive ranges of 174 and 192 km, though not always, and may even appear at the 210 km range. Although not as clearly defined as the marked striations, it should be noted that the striation theme is evident at a later time in the plots. A number of the events have one clearly defined striation while others have multiple striations, which most often are difficult to distinguish as they *blur* into one another (*e.g.*, 192 km range in Figure 3). For such multiple striation cases it is very reasonable to assume that the striations have similar slopes, as can be clearly seen in the paper Haldoupis et al. (2001) for example and, as such, by using the parallel striation theme a representative striation line can be selected as shown in the 192 km range plot in Figure 3.

3.2 Termignon CADI Observations

Angle-of-arrival results for the CADI observations will be presented for both the fixed frequency and ionogram sweep operation modes. The measurements where restricted to virtual heights between 102 and 111 km to confine the analysis to E_s layer heights, and for the ionogram sweep mode to frequencies between 2 and 4 MHz to help eliminate interference. The ionogram mode was more affected by interference than the fixed frequency mode due to the much shorter measurement time (0.4 s for ionogram mode compared to 6.4 s for fixed frequency mode at each frequency). Over longer measurement periods the interference is more noise-like. Both operating modes were used in the drift measurement analysis as both had some potential deficiencies and thus can act complementary.

In Figure 4 the CADI drift measurements for the fixed frequency and ionogram modes are presented. They both cover the time period of the ATI striation presented in Figure 3 and

also the time period of the ionograms presented in Figure 2. Taking the time period to the nearest 10 min, as this is the temporal resolution of the ionogram mode measurements, the period of interest is from 2230 to 2330 UT on 11 July, 1995. The figure ordinates show the azimuth measured in degrees clockwise from geographic north in the top graph, the (horizontal) speed measured in m/s on the middle graph, and the number of *sources* on the bottom graph. A *source* refers to a Doppler bin which corresponds to an ionospheric reflection point (*e.g.*, Cannon et al. (1991); Grant et al. (1995)).

Under the assumption that the E_s layer motions measured in the E-region are controlled by the ambient neutral winds and that these motions will not change quickly over the time periods under consideration, the mean speed and azimuth were calculated from both techniques. As well, the standard deviation of the mean values were calculated as an indication of the reliability of the measurements. For the ionogram mode presented in Figure 4 the mean speed was 19 m/s with a standard deviation of 16 m/s and the mean azimuth was 237° with a standard deviation of 80°. As will be discussed in Section 4.2, the ionogram mode speed values must be discarded; however, the azimuth values are reliable. The mean values for the fixed frequency mode, also shown in Figure 4, were 35 m/s with a standard deviation of 17 m/s and 281° with a standard deviation of 61°.

The mean CADI drift measurements for both the ionogram and fixed frequency modes, along with the corresponding slope of the striations in the ATI plots, were also calculated for the other 7 identified events and the results are listed in Table 1. Next, the benefits and limitations of both measurements will be discussed and then the comparison of the results will be presented.

4 Measurement Techniques and Results

4.1 Valensole HF Radar

The slopes of the striations observed on the ATI plots give a measure of the EW speed or zonal bulk motion. Again, no NS or meridional motions can be estimated from the RTI plots because of the relatively poor range resolution (18 km) of the Valensole radar. Although slightly subjective in their selection, the ATI striation slopes give a fairly accurate estimate of the bulk motion in the zonal direction. To get an estimate of this accuracy, (extreme) values for the ATI striation slopes were determined and it was found that the estimated slopes were within ±5 m/s of the estimated slopes in the most extreme cases and typically much better. It should be noted that the slope may sometimes be better described by piece-wise slopes which would indicate a change in speed of the drift motions over the observation times. However, this is typically seen at large azimuths and likely has more to do with aspect sensitivity conditions and, as such, is ignored in the present study.

4.2 Termignon CADI

CADI instruments have the ability to measure both the speed and azimuth of drifting E_s layer patches in both interferometric modes; that is, the fixed frequency mode or the ionogram seep mode. Typically the fixed frequency mode is usually applied for drift measurements in the F-region. However, the ionosonde can also measure sporadic-E layer drift motions as well by selecting a height range between say $\sim$95 to 115 km (in this study 102 to 111 km was selected to minimise interference). Except now, unlike the situation where there are many reflecting sources spread out with virtual altitude as in the F-region, there are relatively few sources in the narrow layers associated with sporadic-E. This is because CADI has a range resolution of 3 km whereas the E_s layer widths are typically of this order or less (Shen et al. (1976); Smith and Mechty (1972)); thus, there are very few sources, or reflecting levels, as most end up in the same altitude range bin. To help alleviate this problem, all five of the fixed frequency scans were combined together to produce drift measurements. This is the standard technique as all sources are assumed to drift at the same speed and direction (Cannon et al. (1991); Grant et al. (1995) and references therein). This helped but still the number of sources is typically low, that is, only about 10 with E_s present and lower without E_s. As well, there were a couple of events where the CADI could not make meaningful measurements in the fixed frequency mode (see Table 1).

In an effort to increase the number of sources, and hopefully the reliability of the measurements, the angle-of-arrival technique was applied to the ionogram mode. Technically there is functionally no difference between the ionogram and the fixed frequency modes except the ionogram mode is usually set to have a poorer spectral resolution in order to provide a short measurement time at each frequency and thus allow for many frequencies to be included in a sweep. The easy detection of sporadic-E layers with an ionosonde, along with better than usual averaging, allowed for using the ionogram mode in the angle-of-arrival analysis. This greatly increased the number of sources as the ionogram sweep between 2 and 4 MHz included 86 frequencies and then even with only one or two altitude range bins for each frequency the number of sources was easily between one and two hundred. It would have been preferred to use the higher frequencies from the ionogram mode, as will be discussed immediately below, but the interference at these frequencies adversely affected the analysis.

Although the number of sources increased, the spectral information is significantly reduced in the ionogram mode compared to that for the fixed frequency mode and with the relatively low drift velocities associated with the E_s patches, the velocity magnitude information is not valid for the ionogram mode analysis. For example, at 4 MHz the velocity bin size for the ionogram mode is 94 m/s while the typical drift speeds are $\sim$50–100 m/s. As such, the drift speed values determined using the ionogram mode analysis presented in Table 1 should be ignored; however, the azimuth information

determined from the ionogram mode analysis is valid as it does not depend on the spectral resolution.

The phase difference between the antennas of each orthogonal antenna pair, which is used to determine the azimuth, is determined using cross-spectral analysis and as long as the reflected drift signal dominates a given frequency bin (or bins), regardless of the spectral resolution, the phase information will be retained. It is very reasonable to assume, and in fact is the basis for the drift measurement technique, that the reflected drift signal has a relatively strong returned power (and a relatively narrow spectral component) and, as such, dominates the detected signal. A further limitation of the ionogram mode in this study is the rather poor temporal resolution of only once every 10 min. Nonetheless, the results determined using the ionogram mode have certain advantages and thus can help support those obtained using the fixed frequency mode.

In fact, the angle-of-arrival technique implemented in the CADI instruments is essentially the IDI technique commonly used by MF wind radars to measure mesospheric winds (Adams et al. (1985); Adams et al. (1986)). Dynasonde ionosondes in the Antarctic (Jones et al. (1997); Charles and Jones (1999)) and at the Bear Lake Observatory in Utah, U.S.A. (Berkey et al., 2001) have been converted to use the IDI technique to observe the mesospheric wind field at heights from 70 to 105 km. In principle a CADI could measure winds at mesospheric heights as well, but CADI instruments are low-powered ones with simple antennas and some modifications would be required.

4.2.1 Quality of the CADI Data

Now the quality of the CADI data will be further addressed. The fixed frequency observations presented in Figure 4 often show a systematic *up-down* variation of adjacent measurements. This up-down variation is clearly instrumental and typically observed in high-latitude F-region CADI observations and should not be focused upon, but rather the longer-term mean trends should be considered. Recall that CADI has been optimised to measure F-region drifts at high-latitudes where the drift speeds could be up to 1000 m/s and are typically between a few hundred and 600–700 m/s (Grant et al., 1995). For high-latitude F-region measurements the systematic up-down variations are typically 30–50 m/s in agreement with those presented here. Of course, this same type of up-down variation is observed in the azimuth data as well, except high-latitude measurements have a typical variation of $\sim$30° to $\sim$50° while those presented here may be more variable, presumably due to the relatively low number of reflection sources.

The drift speed measurement accuracy is influenced by a number of factors, namely: 1) if the phase is not matched between the antennas of an antenna pair this could affect the drift velocity magnitude, but normally this is only critical for large drift speeds, which do not apply here, and nevertheless phase matching was taken into consideration; 2) the FFT and its frequency resolution is not optimal for measuring the low

drift magnitudes at mid-latitudes, but should be sufficient; 3) averaging can reduce drift speed measurements, but it was essential in helping overcome the effects of man-made interference which adversely affected the absolute values of the drift measurements; and finally, 4) the dominant influence of man-made interference, despite all the efforts to minimise it, would reduce the drift speed magnitude. Clearly points 3) and 4) are significantly related to one another and both can affect the accuracy of the sporadic-E layer drifts.

Everything discussed for the fixed frequency mode drift analysis also applies to the ionogram mode drift analysis as well, except the ionogram mode drift velocity magnitudes (speeds) are not valid (point 2)) as already discussed above. As also discussed above, however, the azimuth component of the ionogram analysis is valid and the averaged values from the two analysis modes presented in Table 1 agree extremely well in 5 out of the 6 events where comparisons can be made. Similar good agreement can be seen in the azimuth plot in Figure 4 as well. The ionogram mode results strongly support the fixed frequency mode results, but only in the azimuth measurement of the drift. Unfortunately, the operating parameters of the ionogram mode and the interference/noise problem resulted in an invalid drift speed measurement for the ionogram mode analysis. As such, this does not allow for the use of the ionogram mode analysis in a comparison with the HF drift measurements, which were only able to measure the drifts in the zonal direction.

Clearly it would have been preferable if CADI had different operating parameters than those selected for the experiment presented here. Ionograms are essential for identification of sporadic-E layers while the higher spectral resolution and noise rejection associated with the fixed frequency mode is needed for more accurate drift measurements. A compromise between the two modes would have been desirable; that is, for example one could increase the number of fixed frequencies to the extent that it has ionogram sweep-like characteristics (*i.e.*, enough frequencies so that E_s can be identified) while retaining a higher degree of spectral resolution in order to get more accurate measurements and to reduce interference.

4.3 Comparison of CADI and HF Radar Drifts

In order to compare the CADI drift measurements with the zonal drifts made by the Valensole radar, the component of CADI drift along the azimuthal direction in the field-of-view of the HF radar must be computed. The CADI drift estimates along the zonal direction are presented in Table 2 together with the drifts measured by the HF radar. Recall that the azimuth direction of the HF radar is not exactly EW but $\sim 255°$ clockwise from north or $\sim 15°$ south of east. As seen, the CADI fixed frequency drifts typically underestimate those calculated from the ATI striation slopes by about 30% or more and that there is reasonably good agreement only for event 8. There are no ionogram mode drifts for comparison as the drift velocity magnitudes are invalid in this mode as discussed in the previous section. The disagreements of the

CADI estimates with the HF zonal speeds are attributable to interference as discussed above. The negative CADI values (eastward drifts) are possibly because these measurements have been adversely affected by interference. Obviously, in these cases the CADI measurements are unreliable.

It is unfortunate that the Valensole HF radar is unable to resolve north-south motions well because of its poor range resolution of 18 km. As such, there could be a significant NS component which went undetected by the HF radar; thus, a full comparison with the CADI measurements is not possible. However, if there was such a NS component it would have been indicated by the azimuth measurements of the CADI, but this was not the case for the events analysed here. The results in Table 1 indicate that the CADI measured drift direction was consistently westward (270° azimuth), which is also typical for the bulk drifts of QP echoes in the premidnight time sector, as reported in a number of studies (Yamamoto et al. (1992); Yamamoto et al. (1994); Tsunoda et al. (1994); Hysell and Burcham (2000); Hysell et al. (2002); Haldoupis et al. (2001); Haldoupis et al. (2003)).

It is recognised that the present CADI measurements of horizontal drifts were not the best as they had been contaminated by strong man-made interference. They were, however, the only ones ever made concurrently with backscatter observations using a coherent radar with the ability to scan a large azimuthal sector and thus being able to measure zonal bulk motions. Nonetheless, this study indicates that applying the CADI drift measurement technique at sporadic-E layer altitudes in the summer nighttime mid-latitude E-region can give information on neutral wind motions. Such measurements are often difficult to obtain at these altitudes. From the present study it is also concluded that the CADI fixed frequency mode analysis results are the most immune to noise and interference whereas the ionogram mode results were only valid for the azimuth measurements due to the noise and interference. Nonetheless, the ionogram mode azimuth measurements did support those from the fixed frequency mode analysis. Finally, for this type of study, the traditional ionograms are essential in identifying the presence of sporadic-E layers.

5 Summary

The large azimuthal extent of the Valensole HF radar was used to measure bulk zonal motions of quasi-periodic echoing regions of mid-latitude sporadic-E layers. The present HF measurements are in agreement with several studies showing that unstable E_s patches in the pre-midnight sector drift mostly westward across the radar field-of-view, presumably with the neutral wind.

Also an angle-of-arrival CADI ionosonde situated under a portion of the field-of-view of the Valensole HF radar was used to measure horizontal drift motions of the unstable E_s layers. In an effort to validate the CADI estimates its drifts were compared with the motions inferred from the azimuth-time-intensity plots of the coherent echoes. The CADI drift

measurements showed reasonable agreement in most events compared to the drifts measured along the azimuthal (EW) direction of the HF radar. It is postulated that the reason for the observed discrepancies between the two sets of measurements was man-made radio interference, which can affect the quality of the CADI data significantly.

It is tentatively concluded that, when properly configured, a CADI ionosonde can be useful in monitoring neutral winds in the mid-latitude E-region by measuring the horizontal drifts of sporadic-E layer patches. In part this requires that the measurements are made under electromagnetically quiet conditions, either by hardware modifications or selection of quiet sites or both, such that the data are free of man-made interference. For a more definitive conclusion, however, it is felt that the CADI drift measurements need to be validated further by means of deploying similar experiments as the one described in the present study.

References

Adams, G. W., D. P. Edwards, and J. W. Brosnahan, The imaging Doppler interferometer: Data Analysis, *Radio Sci., 20*, 1481–1492, 1985.

Adams, G. W., J. W. Brosnahan, D. C. Walden, and S. F. Nerney, Mesospheric observations using a 2.66 MHz radar as an imaging Doppler interferometer: description and first results, *J. Geophys. Res., 91*, 1671–1683, 1986.

Berkey, F. T., C. S. Fish, and G. O. L. Jones, Initial observations of mesospheric winds using IDI radar measurements at the Bear Lake Observatory, *Geophys. Res. Lett., 28*, 135–138, 2001.

Bourdillon, A., C. Haldoupis, and J. Delloue, High-frequency Doppler radar observations of magnetic aspect sensitive irregularities in the midlatitude E region ionosphere, *J. Geophys. Res., 100*, 21,503–21,521, 1995.

Charles, K. and G. O. L. Jones, Mesospheric mean winds and tides observed by the Imaging Doppler Interferometer (IDI) at Halley, Antarctica, *J. Atmos. Terr. Phys., 61*, 351–362, 1999.

Cannon, P. S., B. W. Reinisch, J. Buchau, and T. W. Bullett, Response of the polar cap F region convection direction to changes in the interplanetary magnetic field: Digisonde measurements in Northern Greenland, *J. Geophys. Res., 96*, 1239–1250, 1991.

Grant, I. F., J. W. MacDougall, J. M. Ruohoniemi, W. A. Bristow, G. J. Sofko, J. A. Koehler, D. Danskin, and D. André, Comparison of plasma flow velocities determined by the ionosonde Doppler drift technique, SuperDARN radars, and patch motion, *Radio Sci., 30*, 1537–1549, 1995.

Haldoupis, C., D. T. Farley, and K. Schlegel, Type 1 radar echoes from the midlatitude E region, *Ann. Geophys., 28*, 908–917, 1997.

Haldoupis, C., A. Bourdillon, J. Delloue, and G. C. Hussey, Wavelength dependence of Doppler spectrum broadening in midlatitude E region coherent backscatter, *J. Geophys. Res., 103*, 11,605–11,615, 1998.

Haldoupis, C., G. C. Hussey, A. Bourdillon, and J. Delloue, Azimuth-Time-Intensity striations of quasiperiodic radar echoes from the midlatitude E region ionosphere, *Geophys. Res. Lett., 28*, 1933–1936, 2001.

Haldoupis, C., A. Bourdillon, A. Kamburelis, G. C. Hussey, and J. A. Koehler, 50 MHz continuous wave interferometer observations of the unstable mid-latitude E-region ionosphere, *Ann. Geophys., 21*, 1789–1600, 2003.

Hussey, G. C., J. Delloue, C. Haldoupis, and A. Bourdillon, E-region mid-latitude decametre irregularities observed at four radar frequencies. Experiment and first results, *Ann. Geophys., 15*, 918–924, 1997.

Hussey, G. C., K. Schlegel, and C. Haldoupis, Simultaneous 50-MHz coherent backscatter and digital ionosonde observations in the midlatitude E region, *J. Geophys. Res., 103*, 6991–7001, 1998.

Hussey, G. C., C. Haldoupis, A. Bourdillon, and D. André, Spatial occurrence of decameter midlatitude E region backscatter, *J. Geophys. Res., 104*, 10,071–10,080, 1999.

Hysell, D. L. and J. D. Burcham, The 30-MHz radar interferometer studies of midlatitude E region irregularities, *J. Geophys. Res., 105*, 12,797–12,812, 2000.

Hysell, D. L., M. Yamamoto, and S. Fukao, Imaging radar observations and theory of type I and type II quasiperiodic echoes, *J. Geophys. Res., 107*, ido10.1029/2002JA009292, 2002.

Jones, G. O. L., K. Charles, and M. J. Jarvis, First mesospheric observations using an imaging Doppler interferometer adaptation of the dynasonde at Halley, Antarctica, *Radio Sci., 32*, 2109–2122, 1997.

Kagan, L. M., and M. C. Kelley, A wind-driven gradient drift mechanism for midlatitude E region ionospheric irregularities, *Geophys. Res. Lett., 25*, 4141–4144, 1998.

Larsen, M. F., S. Fukao, M. Yamamoto, R. T. Tsunoda, K. Igarashi, and T. Ono, The SEEK chemical release experiment: Observed neutral wind profile in a region of sporadic-E, *Geophys. Res. Lett., 25*, 1789–1792, 1998.

Pan, C. J., C. H. Liu, J. Röttger, and S. Y. Su, A three dimensional study of E region irregularity patches in the equatorial anomaly using the Chung-Li VHF radar, *Geophys. Res. Lett., 21*, 1763–1766, 1994.

Riggin, D., W. E. Swartz, J. Providakes, and D. T. Farley, Radar studies of long wavelength waves associated with midlatitude sporadic E layers, *J. Geophys. Res., 91*, 8011–8024, 1986.

Shen, J. S., W. E. Swartz, D. T. Farley, and R. M. Harper, Ionization layers in the nighttime E region valley above Arecibo, *J. Geophys. Res., 81*, 5517–5526, 1976.

Six, M., J. Parent, A. Bourdillon, and J. Delloue, A new multibeam receiving equipment for the Valensole skywave HF radar: Description and applications, *IEEE Trans. Geosci. Remote Sens., 34*, 708–719, 1996.

Smith, L. G., and K. L. Mechty, Rocket observations of sporadic E layers, *Radio Sci., 7*, 367–376, 1972.

Tanaka, T., and S. V. Venkateswaran, Characteristics of field-aligned E region irregularities over Ioka ($36°$), Japan, I., *J. Atmos. Terr. Phys., 44*, 395–406, 1982.

Tsunoda, R. T., S. Fukao, and M. Yamamoto, On the origin of quasiperiodic radar backscatter from midlatitude sporadic E, *Radio Sci., 29*, 349–365, 1994.
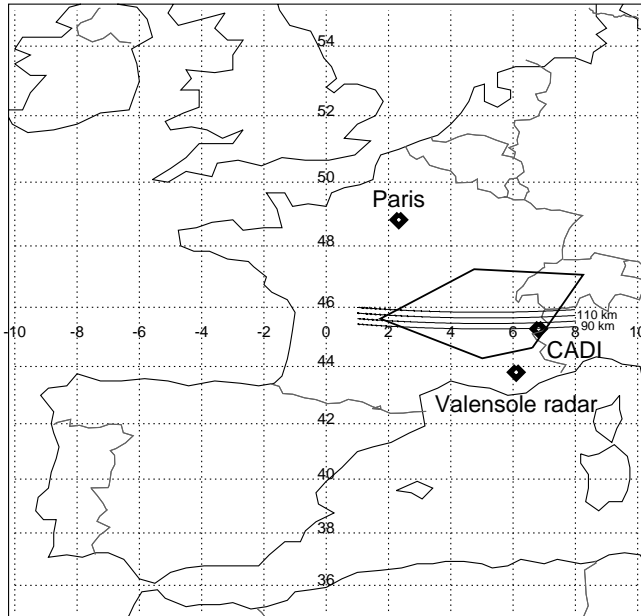
Fig. 1. Map showing the location of the Valensole HF radar and the CADI instrument.
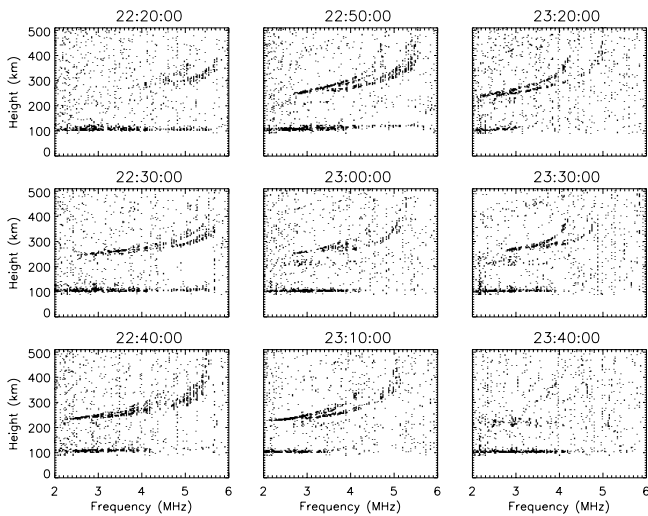

Fig. 2. Ionograms from the period 2220 to 2340 UT on 11 July, 1995. During this period sporadic-E is clearly observed.

Yamamoto, M., S. Fukao, R. F. Woodman, T. Ogawa, T. Tsuda, and S. Kato, Midlatitude E region field-aligned irregularities observed with the MU radar, *J. Geophys. Res., 96,* 15,943–15,949, 1991.

Yamamoto, M., S. Fukao, T. Ogawa, T. Tsuda, and S. Kato, A morphological study on mid-latitude E-region field-aligned irregularities observed with the MU radar, *J. Atmos. Terr. Phys., 54,* 769–777, 1992.

Yamamoto, M., N. Komoda, S. Fukao, R. T. Tsunoda, T. Ogawa, and T. Tsuda, Spatial structure of the E region field-aligned irregularities revealed by the MU radar, *Radio Sci., 29,* 337–347, 1994.
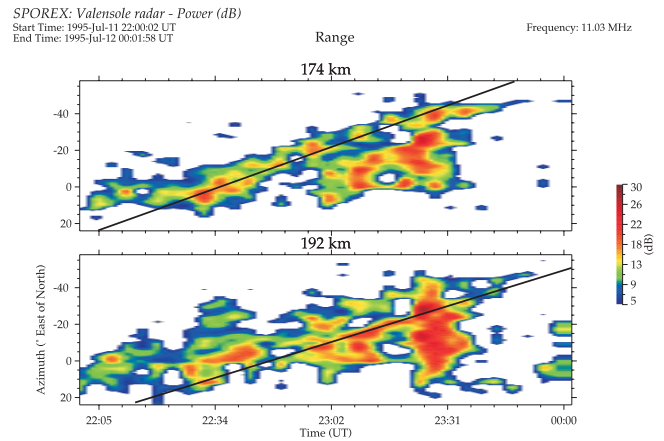

Fig. 3. Azimuth-Time-Intensity (ATI) plot from analysis of Valensole HF coherent backscatter observations. The time period corresponds to that of the ionograms shown in Figure 2. The period of interest is from 2230 to 2330 UT, 11 July, 1995. The striations indicated by the black lines gives an average EW drift of ∼36 m/s.
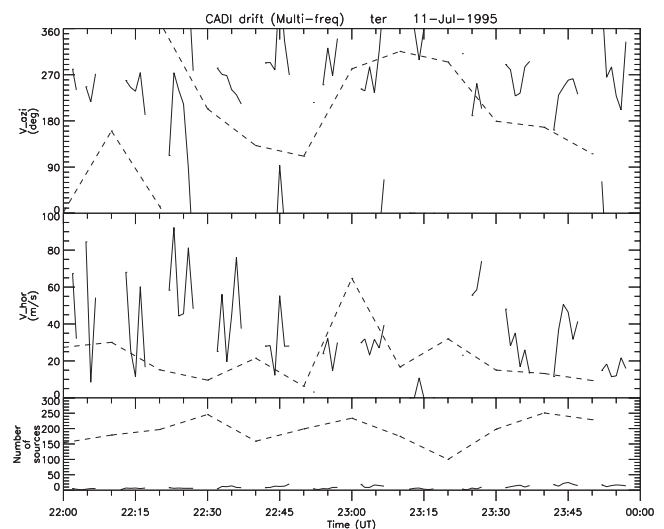

Fig. 4. CADI drift analysis from the same time period as presented in Figures 2 and 3. Again, the period of interest is 2230 to 2330 UT on 11 July, 1995. The solid lines represent the fixed frequency mode drift analysis and the dashed lines represent the ionogram mode drift analysis.

Table 1. Table of the 8 events comparing the drift measurements from the ATI HF radar analysis (EW zonal drifts only) to both the ionogram and fixed frequency mode analysis (drift speed and horizontal direction).

Event	HF radar measurements		CADI measurements				
				ionogram mode		fixed frequency mode	
	time period	speed	time period	speed[†] value(s.d.)	azimuth value(s.d.)	speed value(s.d.)	azimuth value(s.d)
	(UT)	(m/s)	(UT)	(m/s)	(deg)	(m/s)	(deg)
1	6–7 July 2355–0034	67	0000–0030	20(7)	215(56)	—	—
2	7–8 July 2234–2342	62	2230–2340	49(37)[a]	66(97)[a]	—	—
3	8–9 July 2232–2320	38	2230–2320	34(21)	332(77)	36(23)	115(102)[a]
4	8–9 July 2335–0024	60	2330–0030	17(12)	227(119)[a]	31(18)[b] 60(20)[b]	147(59)[b] 247(26)[b]
5	10–11 July 0032–0101	76	0030–0100	22(10)	226(127)[a]	49(20)	249(40)
6	10–11 July 0138–0247	79	0130–0300	30(11)	257(76)	53(27)[c]	290(51)[c]
7	11–12 July 2230–2329	36	2230–2330	19(16)	237(80)	35(17)	281(61)
8	12–13 July 2304–0025	36	2300–0030	29(18)	233(91)	43(25)	228(96)[a]

[†] Speed values for the ionogram mode are invalid. See text for details.
[a] Large variation in either speed or azimuth.
[b] Two clearly defined drift regimes roughly equally divided in time during this interval.
[c] Essentially data from 0130–0200 time interval only.

Table 2. Table of the 8 events comparing the drift measurements in the azimuthal (zonal or EW direction) from the ATI HF radar analysis to the fixed frequency mode analysis.

Event	HF radar measurements	CADI measurements
		fixed frequency mode
	speed	speed
	(m/s)	(m/s)
1	67	—
2	62	—
3	38	-28
4	60	-10[a] 59[a]
5	76	49
6	79	43[b]
7	36	31
8	36	38

[a] Two clearly defined drift regimes roughly equally divided in time during this interval.
[b] Essentially data from 0130–0200 time interval only.